Many-body interferometry of magnetic polaron dynamics

Yuto Ashida, Richard Schmidt, Leticia Tarruell, and Eugene Demler

Phys. Rev. B **97**, 060302 — Published 20 February 2018

DOI: 10.1103/PhysRevB.97.060302

Many-body interferometry of magnetic polaron dynamics

Yuto Ashida,[1] Richard Schmidt,[2,3,4] Leticia Tarruell,[5] and Eugene Demler[3]

[1]*Department of Physics, University of Tokyo, 7-3-1 Hongo, Bunkyo-ku, Tokyo 113-0033, Japan*
[2]*ITAMP, Harvard-Smithonian Center for Astrophysics, Cambridge, Massachusetts 02138, USA*
[3]*Department of Physics, Harvard University, Cambridge, Massachusetts 02138, USA*
[4]*Max-Planck-Institut für Quantenoptik, Hans-Kopfermann-Strasse. 1, 85748 Garching, Germany*
[5]*ICFO-Institut de Ciències Fotòniques, The Barcelona Institute of Science and Technology, 08860 Castelldefels (Barcelona), Spain*

(Dated: February 7, 2018)

The physics of quantum impurities coupled to a many-body environment is among the most important paradigms of condensed matter physics. In particular, the formation of polarons, quasiparticles dressed by the polarization cloud, is key to the understanding of transport, optical response, and induced interactions in a variety of materials. Despite recent remarkable developments in ultracold atoms and solid-state materials, the direct measurement of their ultimate building block, the polaron cloud, has remained a fundamental challenge. We propose and anlalyze a unique platform to probe time-resolved dynamics of polaron-cloud formation with an interferometric protocol. We consider an impurity atom immersed in a two-component Bose-Einstein condensate, where the impurity generates spin-wave excitations that can be directly measured by the Ramsey interference of surrounding atoms. The dressing by spin waves leads to the formation of magnetic polarons and reveals a unique interplay between few- and many-body physics that is signified by single- and multi-frequency oscillatory dynamics corresponding to the formation of many-body bound states. Finally, we discuss concrete experimental implementations in ultracold atoms.

Understanding the role of interactions between an impurity and its environment is a fundamental problem in quantum many-body physics. A central concept for the description of such systems is a "dress" of collective excitations surrounding the impurity, also known as the polaron cloud [1]. It crucially determines thermodynamic and transport properties of a wide variety of condensed matter systems including doped semiconductors [2], metallic ferromagnets [3], high-temperature superconductors [4], ^{3}He-^{4}He mixtures [5], and perovskites [6]. Meanwhile, recent experimental realizations of imbalanced mixtures of ultracold atoms have opened up new possibilities for studying polaron physics in a highly controlled manner. Until now most studies focused on impurities interacting with a single-component Bose-Einstein condensate (BEC) [7–33] or Fermi gas of atoms [34–47]. This allowed to take first steps to explore physics of polaron beyond the Fröhlich paradigm and the Anderson orthogonality catastrophe [48–52]. Despite these remarkable developments, measuring its ultimate building block, the polaron cloud, has remained a challenge not only in ultracold atoms but also in solid-state materials. A major difficulty stemmed from the elusive nature of polaron cloud as it is associated with subtle density change in the environment arising from the interaction with the impurity.

In this Rapid Communication, we show that the use of Ramsey interferometry performed on *bath atoms* can overcome the challenge and allows a direct measurement of polaron-cloud formation in real time. Applying it to impurity atoms immersed in a two-species Bose-Einstein condensate (BEC), we analyze impurities interacting with a magnetic environment and study the impact of polaron-cloud formation on the many-body environment. The setup is illustrated in Fig. 1(a); the host BEC atoms provide an artificial ferromagnetic medium in which the impurity is dressed by spin-wave excitations, leading to the formation of a magnetic polaron. In previous setups [7–19, 21, 24–31], the impurity is coupled only to phonon excitations and observing its cloud formation poses a daunting challenge due to the difficulty to measure a minuscule density change around the impurity. In

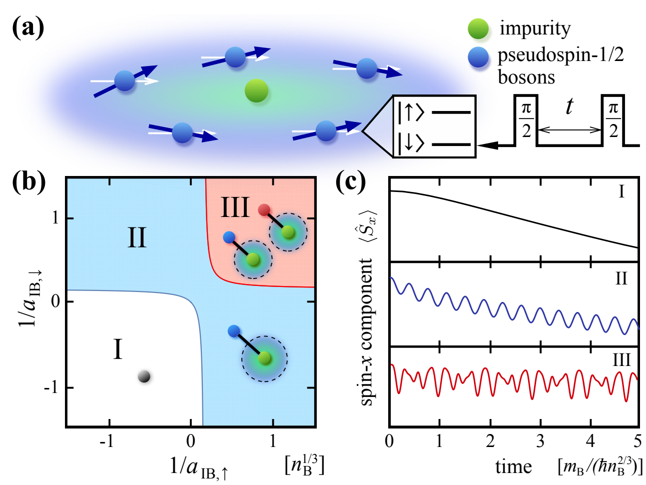

FIG. 1. (color online). (a) Illustration of an impurity atom immersed in a two-component BEC. Arrows indicate the internal pseudospin states of BEC atoms. By applying a $\pi/2$-pulse, the host bosons are initially prepared in an equal superposition of spin ↑- and ↓-state. The interaction between the impurity and host atoms induces spin dephasing, which is measurable by Ramsey interferometry. (b) Depending on the impurity-boson scattering lengths $a_{\mathrm{IB},\uparrow\downarrow}$, the system is characterized by the existence of zero, one, and two many-body bound states (regions I, II, and III). The diagram is plotted for a boson-boson scattering length $a_{\mathrm{BB}}n_{\mathrm{B}}^{1/3} = 0.05$, and $m_{\mathrm{I}}/m_{\mathrm{B}} = 0.95$ as appropriate for a mixture of ^{41}K-^{39}K atoms. (c) The BEC spin dephasing dynamics exhibits (I) monotone relaxation, (II) single- and (III) multi-frequency oscillations reflecting the existence of bound states. The dephasing signal is proportional to the number of impurities, which fixes the scale of the vertical axis.

contrast, a magnetic polaron is dressed by a spin-polarized cloud created from changes in spin configurations [53]. It is this magnetic dressing that enables one to directly measure the polaron cloud by performing Ramsey interferometry on *surrounding atoms*, revealing its rich out-of-equilibrium dynamics. As a striking feature that is not readily attainable in solid-state systems, we find that the polaron cloud is composed of many-body bound states in the strong-coupling regime. This leads to a unique 'phase diagram' of the polaron cloud (Fig. 1(b)), which characterizes distinct oscillatory real-time dynamics in the many-body environment (Fig. 1(c)). Moreover, our scheme can effectively enhance signal amplitudes from the impurity because the impurity creates multiple excitations in the bath that can be directly detected in experiments. This novel protocol can be transferred to a multitude of experimental systems [54–60] in which interferometric schemes are readily available. Our approach thus implies possibilities for enhancing the detectability of impurity physics in a way different from previous studies, where the impurity itself was probed either by radio-frequency [9, 22, 23, 34, 35, 40–42] or interferometric measurements [49–51, 61] and thus the signal amplitudes were intrinsically limited by the number of impurities.

Model.— We consider an impurity of mass $m_{\rm I}$ having no internal degrees of freedom and being immersed in a weakly interacting *two-component* spinor BEC of atoms of mass $m_{\rm B}$ (Fig. 1(a)). The system is described by the Hamiltonian

$$\hat{H} = \hat{H}_{\rm B} + \hat{V}_{\rm IB} + \hat{H}_{\rm I}, \tag{1}$$

where

$$\hat{H}_{\rm B} = \sum_{\mathbf{k}\sigma} \epsilon_{\mathbf{k}} \hat{a}^\dagger_{\mathbf{k}\sigma}\hat{a}_{\mathbf{k}\sigma} + \frac{g_{\rm BB}}{2V}\sum_{\mathbf{k}\mathbf{k}'\mathbf{q}\sigma\sigma'} \hat{a}^\dagger_{\mathbf{k}+\mathbf{q}\sigma}\hat{a}^\dagger_{\mathbf{k}'-\mathbf{q}\sigma'}\hat{a}_{\mathbf{k}'\sigma'}\hat{a}_{\mathbf{k}\sigma} \tag{2}$$

accounts for the background BEC of density $n_{\rm B}$. The interaction between the impurity and the host bosons is given by

$$\hat{V}_{\rm IB} = \frac{1}{V}\sum_{\mathbf{k}\mathbf{q}\sigma} g_{{\rm IB},\sigma}\hat{a}^\dagger_{\mathbf{k}+\mathbf{q}\sigma}\hat{a}_{\mathbf{k}\sigma} e^{i\mathbf{q}\hat{\mathbf{R}}}, \tag{3}$$

and $\hat{H}_{\rm I} = \hat{\mathbf{P}}^2/(2m_{\rm I})$ is the kinetic energy of the impurity. The operators $\hat{a}_{\mathbf{k}\sigma}$ ($\hat{a}^\dagger_{\mathbf{k}\sigma}$) annihilate (create) the host bosons with wavenumber $\mathbf{k}$ and spin $\sigma =\uparrow,\downarrow$, and $\epsilon_{\mathbf{k}} = \hbar^2\mathbf{k}^2/(2m_{\rm B})$ is their dispersion relation. The momentum (position) of the impurity is described by $\hat{\mathbf{P}}$ ($\hat{\mathbf{R}}$). We assume spin independent interactions between the host bosons characterized by the single parameter $g_{\rm BB}$ as realized for many bosonic species [62, 63]. In contrast, the interaction between the impurity and the bosons is spin dependent and given by $g_{{\rm IB},\sigma}$, which are related to the scattering lengths $a_{{\rm IB},\sigma}$ by the Lippmann-Schwinger equation [64].

To realize an effective magnetic environment, we initially prepare a superposition state of the pseudospin-1/2 BEC: $|\Psi_{\rm BEC}\rangle \propto (\hat{a}^\dagger_{\mathbf{0}\uparrow} + \hat{a}^\dagger_{\mathbf{0}\downarrow})^{N_{\rm B}}|0\rangle$, with $N_{\rm B}$ being the number of host bosons. Due to the SU(2) symmetry of $\hat{H}_{\rm B}$, the internal dynamics of the background bosons of homogeneous density causes no decoherence. In contrast, scattering with the impurity breaks this symmetry and induces spin dephasing of the medium. Dealing with a two-component BEC, the collective excitations in the bath correspond not only to phonon ('charge') excitations —as in the case of a single-component BEC— but also spin-wave ('magnon') excitations. The generation of the latter leads to spin dephasing of the medium or, equivalently, dressing of the impurity by magnons. Following the standard procedure of transforming to the frame comoving with the polaron [65], we obtain the effective Hamiltonian [64]:

$$\begin{aligned}\hat{\mathcal{H}} &= g^+_{\rm IB} n_{\rm B} + \frac{(\hat{\mathbf{P}}-\hat{\mathbf{P}}_{\rm B})^2}{2m_{\rm I}} + \sum_{\mathbf{k}}\left(\epsilon^c_{\mathbf{k}}\hat{\gamma}^{\dagger c}_{\mathbf{k}}\hat{\gamma}^c_{\mathbf{k}} + \epsilon^s_{\mathbf{k}}\hat{\gamma}^{\dagger s}_{\mathbf{k}}\hat{\gamma}^s_{\mathbf{k}}\right)\\ &+ \sqrt{\frac{n_{\rm B}}{V}}\sum_{\mathbf{k}}\left[g^+_{\rm IB}W_{\mathbf{k}}\left(\hat{\gamma}^c_{\mathbf{k}} + \hat{\gamma}^{\dagger c}_{-\mathbf{k}}\right) + g^-_{\rm IB}\left(\hat{\gamma}^s_{\mathbf{k}} + \hat{\gamma}^{\dagger s}_{-\mathbf{k}}\right)\right]\\ &+ \frac{g^+_{\rm IB}}{2V}\sum_{\mathbf{k},\mathbf{k}'}\left(V^{(1)}_{\mathbf{k}\mathbf{k}'}\hat{\gamma}^{\dagger c}_{\mathbf{k}}\hat{\gamma}^c_{\mathbf{k}'} + \hat{\gamma}^{\dagger s}_{\mathbf{k}}\hat{\gamma}^s_{\mathbf{k}'} + V^{(2)}_{\mathbf{k}\mathbf{k}'}\hat{\gamma}^{\dagger c}_{\mathbf{k}}\hat{\gamma}^{\dagger c}_{\mathbf{k}'} + {\rm H.c.}\right)\\ &+ \frac{g^-_{\rm IB}}{V}\sum_{\mathbf{k},\mathbf{k}'}\left(u_{\mathbf{k}}\hat{\gamma}^{\dagger s}_{\mathbf{k}'}\hat{\gamma}^c_{\mathbf{k}} - v_{\mathbf{k}}\hat{\gamma}^{\dagger s}_{\mathbf{k}'}\hat{\gamma}^{\dagger c}_{\mathbf{k}} + {\rm H.c.}\right).\end{aligned} \tag{4}$$

Here, $\hat{\mathbf{P}}$ in this frame represents the total momentum of the system (we consider the case $\hat{\mathbf{P}} = 0$ hereafter), $\hat{\mathbf{P}}_B = \sum_{\mathbf{k}}\hbar\mathbf{k}(\hat{\gamma}^{\dagger c}_{\mathbf{k}}\hat{\gamma}^c_{\mathbf{k}} + \hat{\gamma}^{\dagger s}_{\mathbf{k}}\hat{\gamma}^s_{\mathbf{k}})$, $\epsilon^c_{\mathbf{k}} = \sqrt{\epsilon_{\mathbf{k}}(\epsilon_{\mathbf{k}} + 2g_{\rm BB}n_{\rm B})}$ and $\epsilon^s_{\mathbf{k}} = \hbar^2\mathbf{k}^2/(2m_{\rm B})$ are the total boson momentum and the dispersion relations of the charge and spin wave excitations, respectively. The excitations are annihilated (created) by the operators, $\hat{\gamma}^{c,s}_{\mathbf{k}}$ ($\hat{\gamma}^{\dagger c,s}_{\mathbf{k}}$) that obey the commutation relations $[\hat{\gamma}^\xi_{\mathbf{k}}, \hat{\gamma}^\eta_{\mathbf{k}'}] = [\hat{\gamma}^{\dagger\xi}_{\mathbf{k}}, \hat{\gamma}^{\dagger\eta}_{\mathbf{k}'}] = 0$, and $[\hat{\gamma}^\xi_{\mathbf{k}}, \hat{\gamma}^{\dagger\eta}_{\mathbf{k}'}] = \delta_{\xi,\eta}\delta_{\mathbf{k},\mathbf{k}'}$ with $\xi,\eta = s,c$. We introduce the vertices $W_{\mathbf{k}} = \sqrt{\epsilon_{\mathbf{k}}/\epsilon^c_{\mathbf{k}}}$, $V^{(1)}_{\mathbf{k}\mathbf{k}'} \pm V^{(2)}_{\mathbf{k}\mathbf{k}'} = (W_{\mathbf{k}}W_{\mathbf{k}'})^{\pm1}$, as well as $u_{\mathbf{k}}$ and $v_{\mathbf{k}}$ as the coefficients of the Bogoliubov transformation. We also introduce the average and difference of the interaction parameters as $g^\pm_{\rm IB} = (g_{{\rm IB},\uparrow} \pm g_{{\rm IB},\downarrow})/2$. When $g^-_{\rm IB} \neq 0$, the imbalance in the impurity-boson interactions switches on spin-charge interactions and generates spin waves. While the first two lines in Eq. (4) describe the generalization of Fröhlich polaron-type physics [66] to magnon dynamics, the last two lines account for the strong coupling physics that leads to the formation of magnetic polaron bound states.

Interferometry.— The real-time dynamics of the polaron cloud can be probed through Ramsey interference of bath atoms. Starting with a bath in the $\uparrow$ state, a first $\pi/2$ pulse is used to prepare a superposition of $\uparrow$ and $\downarrow$ as described above. After the system has evolved for a time t, an additional $\pi/2$ pulse is applied and the population $N_\uparrow$ of bath atoms remaining in the $\uparrow$ state after the Ramsey protocol is measured. This directly gives the value of the spin-excitation number $N^s(t) = \sum_{\mathbf{k}}\langle\hat{\gamma}^{\dagger s}_{\mathbf{k}}\hat{\gamma}^s_{\mathbf{k}}\rangle$. One can thus explicitly determine the number $N^s(t)$ of spin-wave excitations in the polaron cloud by measuring the atomic population $N_\uparrow$ after the

Ramsey sequence. While we so far analyze the case of a single impurity, our results can be applied to a finite density of impurities as long as the impurity density is sufficiently low such that impurity-impurity interactions remain negligible, as realizable in experimental systems. The interferometric signal $N^s = N_\uparrow$ is then proportional to the number of impurities and can take a value approaching even a substantial fraction of bath atoms such that it is readily detectable with the current techniques [49–51, 61]. This allows a precise and time-resolved determination of the number of excitations generated in the polaron cloud, which has been challenging to achieve in the previous setups [7–19, 21, 24–31].

Quantum spin dynamics.— The formation of magnetic polarons leads to distinct quantum dynamics of the polaron cloud. To demonstrate this, we invoke the time-dependent variational approach [67]. In particular, we employ a projection onto the submanifold of the Hilbert space spanned by the product of coherent states

$$|\Psi(t)\rangle = e^{\sum_{\mathbf{k}}(\alpha^c_{\mathbf{k}}(t)\hat{\gamma}^c_{\mathbf{k}}+\alpha^s_{\mathbf{k}}(t)\hat{\gamma}^s_{\mathbf{k}}-\text{h.c.})}|0\rangle, \qquad (5)$$

where $\alpha^{c,s}_{\mathbf{k}}(t)$ are the time-dependent amplitudes of the charge and spin excitations and $|0\rangle$ is their vacuum. The state (5) gives the exact solution for an impurity of infinite mass immersed into an ideal BEC regardless of the interaction strength between the impurity and host bosons. The equations of motion for $\alpha^{c,s}_{\mathbf{k}}$ are given by the variational condition $\delta[\langle\Psi|i\hbar\partial_t - \hat{\mathcal{H}}|\Psi\rangle] = 0$, which results in the coupled integral equations [64]:

$$i\hbar\partial_t \begin{pmatrix}\alpha^c\\ \alpha^s\end{pmatrix} = \mathcal{M}\begin{pmatrix}\alpha^c\\ \alpha^s\end{pmatrix} + \mathcal{F}, \qquad (6)$$

where the matrix $\mathcal{M}$ and vector $\mathcal{F}$ are independent of $\alpha^{c,s}_{\mathbf{k}}$. The stationary solution $|\Psi_{\text{mpol}}\rangle$ of Eq. (6) contains nonzero spin and charge excitations and represents the magnetic dressed polaron with energy $E_{\text{mpol}} = \langle\Psi_{\text{mpol}}|\hat{\mathcal{H}}|\Psi_{\text{mpol}}\rangle$.

Figure 2 shows the number of spin and charge excitations $N^{s,c}(t)$ for different scattering lengths $a_{\text{IB},\sigma}$ in the regions I, II, and III, where the system supports zero, one, and two bound states (Fig. 1(b)). In the absence of bound states, while $N^c(t)$ eventually saturates, $N^s(t)$ grows as $\propto \sqrt{t}$ and easily exceeds one (panel I in Fig. 2). As a consequence, the observable signals $N^s = N_\uparrow$ can significantly surpass the number of impurities. In contrast, in the conventional measurements acting on the impurity [9, 22, 23, 34, 35, 40–42, 49, 50, 61], the number of detectable signals are strictly limited by that of impurities. In this regard, interferometric probes acting on the environment can provide a new way to effectively enhance experimental signatures of impurities.

The unbounded generation of spin waves originates from the quadratic nature of the magnon dispersion relation [64]. Importantly, collective excitations having quadratic low-energy dispersion ubiquitously appear in many other setups such as fermionic gases [54, 55], multi-component Bose-Einstein condensates [56, 57], and Rydberg or dipolar gases [58–60]. This implies a wide applicability of our protocol because interferometric tools of atomic spectroscopy are readily available in these vastly different systems.

Magnetic dressed bound states.— The presence of bound states triggers single- and multi-frequency oscillations in the number of the spin and charge excitations (panels II and III in Fig. 2). These two different oscillatory dynamics reflect the formation and coupling of many-body bound states, respectively. To gain further insights, we consider the variational wavefunction

$$|\Psi_{\text{b}}(t)\rangle = \sum_{\mathbf{k}}\left(\psi^c_{\mathbf{k}}(t)\hat{\gamma}^{\dagger c}_{\mathbf{k}} + \psi^s_{\mathbf{k}}(t)\hat{\gamma}^{\dagger s}_{\mathbf{k}}\right)|\Psi_{\text{mpol}}\rangle, \qquad (7)$$

which accounts for bound states consisting of single spin-charge excitations bound to the magnetic polaron, i.e., the collective object of the impurity dressed by surrounding many-body excitations. We determine the eigenmodes $\psi^{c,s}_{\mathbf{k}} \propto e^{-i\omega t}$ of the equation of motion for the state (7) which yields the eigenvalue equation [64]

$$(a^-_{\text{IB}})^2 = \left[a^+_{\text{IB}} - l_s(\omega, a^+_{\text{IB}})\right]\left[a^+_{\text{IB}} - l_c(\omega, a^+_{\text{IB}})\right]. \qquad (8)$$

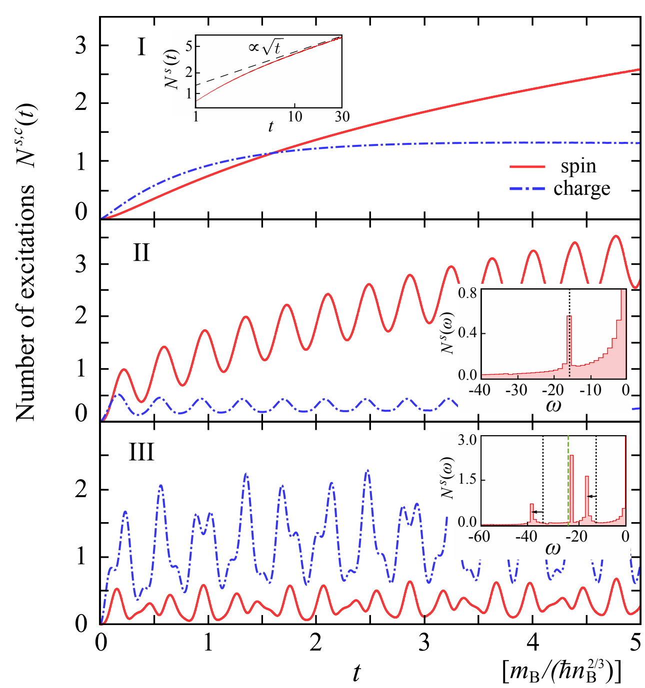

FIG. 2. (color online). Quantum dynamics of bath spin (red solid line) and charge (blue dashed line) excitations for a single impurity immersed in a two-component BEC. The impurity-boson scattering lengths are $n_B^{1/3}(a_{\text{IB},\uparrow}, a_{\text{IB},\downarrow}) = (-1,-10)$ in I, $(3.5,-5)$ in II, and $(3.5, 5)$ in III. The inset in I shows the long-time behavior of spin excitations approaching an asymptotic $\sqrt{t}$ scaling. The insets in II and III show the Fourier spectra of $N^s(t)$. The energies of the underlying bound states and their difference, calculated from Eq. (8), are shown as black dotted lines and green dashed lines, respectively.

Here $a_{\rm IB}^{\pm} = (a_{{\rm IB},\uparrow} \pm a_{{\rm IB},\downarrow})/2$ and $1/l_{s,c} = (2\pi/m_{\rm red})(2m_{\rm red}\sum_{\mathbf{k}}(1/\mathbf{k}^2) + \hbar^2\Pi_{s,c})$, which, together with

$$\Pi_s=\sum_{\mathbf{k}}\frac{1}{\hbar\omega-E_{\rm mpol}-\Omega^s_{\mathbf{k}}},\ \Pi_c=\sum_{\mathbf{k}}\frac{(W_{\mathbf{k}}^2+W_{\mathbf{k}}^{-2})/2}{\hbar\omega-E_{\rm mpol}-\Omega^c_{\mathbf{k}}},\quad (9)$$

are fully regularized expressions ($\Omega^{s,c}_{\mathbf{k}} = \hbar^2\mathbf{k}^2/(2m_{\rm I}) + \epsilon^{s,c}_{\mathbf{k}}$). Depending on the scattering lengths $a_{{\rm IB},\sigma}$, Eq. (8) has zero, one, or two solutions determining the phase boundaries in Fig. 1(b). These boundaries are modified with respect to the corresponding two-body problem as a result of the many-body character of the bound states. In the two-particle problem, a dimer bound state of energy $\epsilon_{\rm dim} = \hbar^2/(2m_{\rm red}a^2_{{\rm IB},\sigma})$ ($m_{\rm red} = m_{\rm I}m_{\rm B}/(m_{\rm I}+m_{\rm B})$) exists for each positive scattering length $a_{{\rm IB},\sigma}$. As a result, there are four distinct regions corresponding to the presence or absence of each bound state, i.e., the impurity bound to a host $\uparrow$- or $\downarrow$-boson. Remarkably, the many-body phase diagram in Fig. 1(b) does not show the corresponding four distinct regimes. Instead, the exchange of magnetic excitations hybridizes the bound states with the medium, resulting in a unified region II.

In this region II, we find that the oscillation frequency governing the bath-spin dynamics agrees with the bound-state energy calculated from Eq. (8) (inset of panel II in Fig. 2). In contrast, in region III, the bath-induced coupling between the two bound states manifests itself as a shift in the oscillation frequencies from the bare bound-state energies and also as a large peak at the difference of the two energies (inset of panel III in Fig. 2). This effect can be understood as a polaronic nonlinearity introduced by the magnetic medium [68], which induces strongly coupled oscillators dynamics, analogous to polariton-polariton interactions [69] and competing orders in strongly correlated electrons [70]. As we depart from the strongly interacting regime, the coupling of the two bound states weakens and the oscillation frequencies eventually converge to the bare bound-state energies given by Eq. (8) [64].

Experimental implementation.— A large number of Bose-Bose and Bose-Fermi mixtures allow for the observation of magnetic polaron physics. As one possible example, we consider here a Bose-Bose mixture of ^{41}K-^{39}K atoms. We identify two miscible states $|\uparrow\rangle = |F=1, m_F=1\rangle$ and $|\downarrow\rangle = |F=1, m_F=0\rangle$ of ^{41}K as the host bosons and $|i\rangle = |F=1, m_F=1\rangle$ of ^{39}K as the impurity. In this case, the $|\uparrow\rangle - |i\rangle$ interaction can be tuned using a Feshbach resonance at 500 G [71]. The imbalance in the scattering lengths of the two-component host bosons is less than 0.4% [72]. While such a small breaking of the SU(2) symmetry can in general induce decoherence of the atomic spins, we confirmed that the effect is negligible compared with the spin dynamics induced by the impurities [64].

In Fig. 3, we plot the energy $\omega_{\rm bound}$ of the magnetic-dressed bound state as calculated from Eq. (8). The result is shown in the vicinity of a Feshbach resonance where $a_{{\rm IB},\uparrow}$ takes a large positive value, while $a_{{\rm IB},\downarrow}$ is determined by a small, positive background value. As shown in the inset of Fig. 3, this significant imbalance in scattering lengths creates

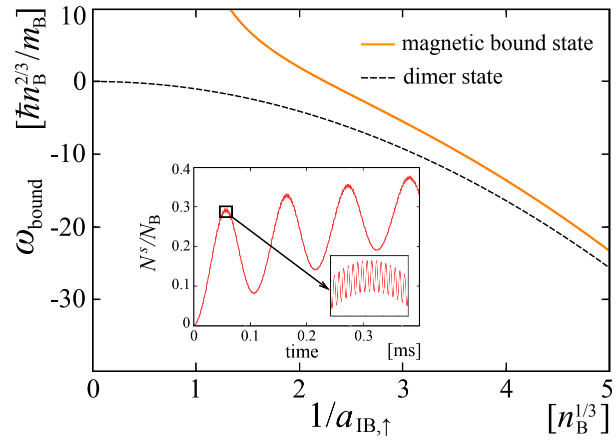

FIG. 3. (color online). The magnetic bound-state energy $\omega_{\rm bound}$ (solid line) calculated from Eq. (8), and the bare dimer energy $\epsilon_{\rm dim} = \hbar^2/(2m_{\rm red}a^2_{{\rm IB},\uparrow})$ (dashed line) are plotted against the inverse impurity-bath scattering length $1/a_{{\rm IB},\uparrow}$. The inset shows the dynamics of spin excitations at $1/(a_{{\rm IB},\uparrow}n_{\rm B}^{1/3}) = 2$ where we assume a homogeneous density $n_{\rm B} = 10^{14}$ cm^{-3}, and a finite impurity density $n_{\rm I}/n_{\rm B} = 0.1$. We choose $a_{\rm BB}n_{\rm B}^{1/3} = 0.05$, and set $1/(a_{{\rm IB},\downarrow}n_{\rm B}^{1/3}) = 15$ and $m_{\rm I}/m_{\rm B} = 0.95$ as appropriate for a ^{41}K-^{39}K mixture.

a large number of observable excitations $N^s(t)$ in the bath, which can exceed the number of impurities. Here we note that the large spin-excitation number $N^s(t)$ is a direct measurable quantity in the proposed Ramsey protocol and can reach to $O(10^4)$ for a typical number $N_{\rm B} = 10^5$ and small, relative impurity density $n_{\rm I}/n_{\rm B} = 0.1$. Moreover, the underlying shallow bound state triggers oscillatory dynamics whose frequency is characterized by the bound-state energy that can be typically ~ 10 kHz, which should be detectable in the time resolution realized in the current experiments [50]. While this oscillation frequency corresponds to a temperature scale $T/k_{\rm B} \simeq 500$ nK that has been already achieved in several experiments [50, 73, 74], we note that our predictions should be accessible in higher temperatures by, for example, localizing the impurities around the center of the system [50] or by performing local measurements [52]. We note that there are also other candidates for bath atoms such as ^{87}Rb and ^{23}Na, where the imbalance in the scattering lengths can be small enough to observe the predicted phenomena [62–64].

Conclusions and Outlook.— We showed that the real-time dynamics of the polaron cloud can be directly probed by employing many-body Ramsey interferometry of bath atoms around the impurity. Analyzing an impurity immersed in a two-component Bose gas, we demonstrated that the generation of spin excitations is the key signature of magnetic-polaron formation and found unique out-of-equilibrium dynamics in the strong-coupling regime such as the characteristic oscillatory behavior governed by the underlying bound states. Our protocol acting on the environment rather than the impurity itself can effectively enhance signal amplitudes of impurities owing to a generation of multiple observable excitations (per impurity) in the environment. This leads to a novel route for observing few-body physics beyond conventional spectroscopy [9, 22, 23] and loss measurements [75] whose signal amplitudes are intrinsically limited by the number of impurities. A generalization to large spin spinor BECs [76] and the use of in-$situ$ imaging techniques [77–81] can provide new insights in polaron physics. It remains an open question to clarify the role of magnon-mediated interaction [82], potentially leading to an instability of fermionic gases.

Acknowledgements.— We acknowledge F. Grusdt, Y. Shchadilova, M. Tomza, M. Ueda, G. Zaránd for fruitful discussions. The authors acknowledge support from the NSF Grant No. DMR-1308435, Harvard-MIT CUA, AFOSR New Quantum Phases of Matter MURI, the ARO-MURI on Atomtronics, ARO MURI Quism program. Y.A. acknowledges support from the Japan Society for the Promotion of Science through Program for Leading Graduate Schools (ALPS) and Grant No. JP16J03613, and Harvard University for hospitality, where this work was completed. R.S. is supported by the NSF through a grant for the Institute for Theoretical Atomic, Molecular, and Optical Physics at Harvard University and the Smithsonian Astrophysical Observatory. L.T. acknowledges support from Fundació Cellex, Spanish MINECO (FIS2014-59546-P and SEV-2015-0522) and EU (PCIG13-GA-2013 No. 631633 and H2020-FETPROACT-2014 No. 641122).

[1] G. Mahan, *Many-Particle Physics* (Kluwer Academic/Plenum Publishers, New York, 2000).
[2] T. Jungwirth, J. Sinova, J. Mašek, J. Kučera, and A. H. MacDonald, Rev. Mod. Phys. **78**, 809 (2006).
[3] P. Majumdar and P. B. Littlewood, Nature **395**, 479 (1998).
[4] E. K. H. Salje, A. S. Alexandrov, and W. Y. Liang, eds., *Polarons and Bipolarons in High Temperature Superconductors and Related Materials* (Cambridge University Press, Cambridge, 2005).
[5] J. Bardeen, G. Baym, and D. Pines, Phys. Rev. **156**, 207 (1967).
[6] J. M. De Teresa, M. R. Ibarra, P. A. Algarabel, C. Ritter, C. Marquina, J. Blasco, J. Garcia, A. del Moral, and Z. Arnold, Nature **386**, 256 (1997).
[7] L. Mathey, D. W. Wang, W. Hofstetter, M. D. Lukin, and E. Demler, Phys. Rev. Lett. **93**, 120404 (2004).
[8] S. Palzer, C. Zipkes, C. Sias, and M. Köhl, Phys. Rev. Lett. **103**, 150601 (2009).
[9] C.-H. Wu, J. W. Park, P. Ahmadi, S. Will, and M. W. Zwierlein, Phys. Rev. Lett. **109**, 085301 (2012).
[10] F. M. Cucchietti and E. Timmermans, Phys. Rev. Lett. **96**, 210401 (2006).
[11] A. Klein, M. Bruderer, S. R. Clark, and D. Jaksch, New J. Phys. **9**, 411 (2007).
[12] J. Tempere, W. Casteels, M. K. Oberthaler, S. Knoop, E. Timmermans, and J. T. Devreese, Phys. Rev. B **80**, 184504 (2009).
[13] W. Casteels, J. Tempere, and J. T. Devreese, Phys. Rev. A **84**, 063612 (2011).
[14] N. Spethmann, F. Kindermann, S. John, C. Weber, D. Meschede, and A. Widera, Phys. Rev. Lett. **109**, 235301 (2012).
[15] W. Casteels, J. Tempere, and J. T. Devreese, Phys. Rev. A **88**, 013613 (2013).
[16] S. P. Rath and R. Schmidt, Phys. Rev. A **88**, 053632 (2013).
[17] W. Li and S. Das Sarma, Phys. Rev. A **90**, 013618 (2014).
[18] R. S. Christensen, J. Levinsen, and G. M. Bruun, Phys. Rev. Lett. **115**, 160401 (2015).
[19] L. A. P. Ardila and S. Giorgini, Phys. Rev. A **92**, 033612 (2015).
[20] L. A. P. n. Ardila and S. Giorgini, Phys. Rev. A **94**, 063640 (2016).
[21] J. Levinsen, M. M. Parish, and G. M. Bruun, Phys. Rev. Lett. **115**, 125302 (2015).
[22] M.-G. Hu, M. J. Van de Graaff, D. Kedar, J. P. Corson, E. A. Cornell, and D. S. Jin, Phys. Rev. Lett. **117**, 055301 (2016).
[23] N. B. Jørgensen, L. Wacker, K. T. Skalmstang, M. M. Parish, J. Levinsen, R. S. Christensen, G. M. Bruun, and J. J. Arlt, Phys. Rev. Lett. **117**, 055302 (2016).
[24] Y. E. Shchadilova, R. Schmidt, F. Grusdt, and E. Demler, Phys. Rev. Lett. **117**, 113002 (2016).
[25] F. Grusdt, Y. E. Shchadilova, a. N. Rubtsov, and E. Demler, Sci. Rep. **5**, 12124 (2015).
[26] J. Vlietinck, W. Casteels, K. Van Houcke, J. Tempere, J. Ryckebusch, and J. T. Devreese, New J. Phys. **17**, 33023 (2015).
[27] R. Schmidt and M. Lemeshko, Phys. Rev. Lett. **114**, 203001 (2015).
[28] A. G. Volosniev, H.-W. Hammer, and N. T. Zinner, Phys. Rev. A **92**, 023623 (2015).
[29] Y. E. Shchadilova, F. Grusdt, A. N. Rubtsov, and E. Demler, Phys. Rev. A **93**, 043606 (2016).
[30] R. Schmidt and M. Lemeshko, Phys. Rev. X **6**, 011012 (2016).
[31] R. Schmidt, H. R. Sadeghpour, and E. Demler, Phys. Rev. Lett. **116**, 105302 (2016).
[32] F. F. Bellotti, T. Frederico, M. T. Yamashita, D. V. Fedorov, A. S. Jensen, and N. T. Zinner, New J. Phys. **18**, 043023 (2016).
[33] B. Midya, M. Tomza, R. Schmidt, and M. Lemeshko, Phys. Rev. A **94**, 041601 (2016).
[34] A. Schirotzek, C.-H. Wu, A. Sommer, and M. W. Zwierlein, Phys. Rev. Lett. **102**, 230402 (2009).
[35] S. Nascimbène, N. Navon, K. J. Jiang, L. Tarruell, M. Teichmann, J. McKeever, F. Chevy, and C. Salomon, Phys. Rev. Lett. **103**, 170402 (2009).
[36] X. Cui and H. Zhai, Phys. Rev. A **81**, 041602 (2010).
[37] R. Schmidt and T. Enss, Phys. Rev. A **83**, 063620 (2011).
[38] P. Massignan and G. M. Bruun, Eur. Phys. J. D **65**, 83 (2011).
[39] R. Schmidt, T. Enss, V. Pietilä, and E. Demler, Phys. Rev. A **85**, 021602 (2012).
[40] M. Koschorreck, D. Pertot, E. Vogt, B. Frohlich, M. Feld, and M. Köhl, Nature **485**, 619 (2012).
[41] C. Kohstall, M. Zaccanti, M. Jag, A. Trenkwalder, P. Massignan, G. M. Bruun, F. Schreck, and R. Grimm, Nature **485**, 615 (2012).
[42] Y. Zhang, W. Ong, I. Arakelyan, and J. E. Thomas, Phys. Rev. Lett. **108**, 235302 (2012).
[43] C. J. M. Mathy, M. B. Zvonarev, and E. Demler, Nature Phys. **8**, 881 (2012).
[44] P. Massignan, M. Zaccanti, and G. M. Bruun, Rep. Prog. Phys. **77**, 034401 (2014).
[45] W. Yi and X. Cui, Phys. Rev. A **92**, 013620 (2015).
[46] W. Ong, C. Cheng, I. Arakelyan, and J. E. Thomas, Phys. Rev. Lett. **114**, 110403 (2015).
[47] F. Meinert, M. Knap, E. Kirilov, K. Jag-Lauber, M. B. Zvonarev, E. Demler, and H.-C. Nägerl, arXiv:1608.08200 (2016).
[48] M. Knap, A. Kantian, T. Giamarchi, I. Bloch, M. D. Lukin, and E. Demler, Phys. Rev. Lett. **111**, 147205 (2013).

[49] M. Cetina, M. Jag, R. S. Lous, J. T. M. Walraven, R. Grimm, R. S. Christensen, and G. M. Bruun, Phys. Rev. Lett. **115**, 135302 (2015).
[50] M. Cetina, M. Jag, R. S. Lous, I. Fritsche, J. T. M. Walraven, R. Grimm, J. Levinsen, M. M. Parish, R. Schmidt, M. Knap, and E. Demler, Science **354**, 96 (2016).
[51] R. Schmidt, M. Knap, D. A. Ivanov, J.-S. You, M. Cetina, and E. Demler, Rep. Prog. Phys. **81**, 024401 (2018).
[52] F. Scazza, G. Valtolina, P. Massignan, A. Recati, A. Amico, A. Burchianti, C. Fort, M. Inguscio, M. Zaccanti, and G. Roati, Phys. Rev. Lett. **118**, 083602 (2017).
[53] P. G. de Gennes, Phys. Rev. **118**, 141 (1960).
[54] A. Mazurenko, C. S. Chiu, G. Ji, M. F. Parsons, M. Kanász-Nagy, R. Schmidt, F. Grusdt, E. Demler, D. Greif, and M. Greiner, Nature **545**, 462 (2017).
[55] G. Valtolina, F. Scazza, A. Amico, A. Burchianti, A. Recati, T. Enss, M. Inguscio, M. Zaccanti, and G. Roati, Nature Phys. **13**, 704 (2017).
[56] A. V. Gorshkov, M. Hermele, V. Gurarie, C. Xu, P. S. Julienne, J. Ye, P. Zoller, E. Demler, M. D. Lukin, and A. M. Rey, Nature Phys. **6**, 289 (2010).
[57] G. E. Marti, A. MacRae, R. Olf, S. Lourette, F. Fang, and D. M. Stamper-Kurn, Phys. Rev. Lett. **113**, 155302 (2014).
[58] J. Zeiher, R. Van Bijnen, P. Schauß, S. Hild, J.-y. Choi, T. Pohl, I. Bloch, and C. Gross, Nature Phys. **12**, 1095 (2016).
[59] F. Böttcher, A. Gaj, K. M. Westphal, M. Schlagmüller, K. S. Kleinbach, R. Löw, T. C. Liebisch, T. Pfau, and S. Hofferberth, Phys. Rev. A **93**, 032512 (2016).
[60] D. Petrosyan, New J. Phys. **19**, 033001 (2017).
[61] M. M. Parish and J. Levinsen, Phys. Rev. B **94**, 184303 (2016).
[62] E. G. M. van Kempen, S. J. J. M. F. Kokkelmans, D. J. Heinzen, and B. J. Verhaar, Phys. Rev. Lett. **88**, 093201 (2002).
[63] C. Samuelis, E. Tiesinga, T. Laue, M. Elbs, H. Knöckel, and E. Tiemann, Phys. Rev. A **63**, 012710 (2000).
[64] See Supplemental Material for details about the derivations and experimental implementations.
[65] T. Lee, F. Low, and D. Pines, Phys. Rev. **341**, 297 (1953).
[66] H. Fröhlich, Adv. Phys. **3**, 325 (1954).
[67] R. Jackiw and A. Kerman, Phys. Lett. A **71**, 1 (1979).
[68] S. Aubry, Physica D **103**, 201 (1997).
[69] N. A. Gippius, I. A. Shelykh, D. D. Solnyshkov, S. S. Gavrilov, Y. G. Rubo, A. V. Kavokin, S. G. Tikhodeev, and G. Malpuech, Phys. Rev. Lett. **98**, 236401 (2007).
[70] S. Pathak, V. B. Shenoy, M. Randeria, and N. Trivedi, Phys. Rev. Lett. **102**, 027002 (2009).
[71] Note that our calculation does not take into account finite range effects, which might become important for this particular resonance.
[72] M. Tomza, Private communications.
[73] F. Fang, R. Olf, S. Wu, H. Kadau, and D. M. Stamper-Kurn, Phys. Rev. Lett. **116**, 095301 (2016).
[74] R. J. Fletcher, R. Lopes, J. Man, N. Navon, R. P. Smith, M. W. Zwierlein, and Z. Hadzibabic, Science **355**, 377 (2017).
[75] P. Naidon and S. Endo, Rep. Prog. Phys. **80**, 056001 (2017).
[76] D. M. Stamper-Kurn and M. Ueda, Rev. Mod. Phys. **85**, 1191 (2013).
[77] W. S. Bakr, J. I. Gillen, A. Peng, S. Fölling, and M. Greiner, Nature **462**, 74 (2009).
[78] J. F. Sherson, C. Weitenberg, M. Endres, M. Cheneau, I. Bloch, and S. Kuhr, Nature **467**, 68 (2010).
[79] Y. Ashida and M. Ueda, Phys. Rev. Lett. **115**, 095301 (2015).
[80] Y. Ashida and M. Ueda, Opt. Lett. **41**, 72 (2016).
[81] A. Alberti, C. Robens, W. Alt, S. Brakhane, M. Karski, R. Reimann, A. Widera, and D. Meschede, New J. Phys. **18**, 053010 (2016).
[82] P. Naidon, arXiv:1607.04507 (2016).